Theor Appl Climatol
DOI 10.1007/s00704-015-1389-y

ORIGINAL PAPER

The Modified Rainfall Anomaly Index (mRAI)—is this an alternative to the Standardised Precipitation Index (SPI) in evaluating future extreme precipitation characteristics?

Stephanie Hänsel · Anne Schucknecht · Jörg Matschullat

Received: 22 February 2013 / Accepted: 19 January 2015

Abstract Precipitation extremes affect various economic sectors and may result in substantial costs for societies. Future projections of such extreme occurrences are needed to successfully develop robust regional adaptation strategies. Model ensemble-based approaches provide a higher level of confidence since they compensate to some degree for the uncertainties of individual climate model projections. An ensemble of twelve regional climate projections from five regional climate models was used to evaluate the suitability of a modified version of the Rainfall Anomaly Index (mRAI) as an alternative to the Standardised Precipitation Index (SPI) in assessing future precipitation conditions. We compared frequency distributions and trends of the mRAI with the SPI for a test region that is climatologically representative of Central Eastern Europe. Both indices are highly correlated with each other at all tested timescales—both for stations and for regionally averaged data—with Pearson correlation coefficients >>0.9 and Spearman correlation coefficients >0.99. There are no significant differences in their frequency distributions, although the mRAI shows slightly higher frequencies in the classes of 'moderately dry' to 'very dry' conditions. The change signals revealed by SPI and mRAI are very similar for mean changes as well as for changes in the extremes. Considering the large bandwidth of change signals of individual regional climate projections, the mRAI provides sufficiently robust results for the evaluation of future precipitation anomaly trends. The notably more complex calculation of the SPI has no appreciable advantage for this application.

S. Hänsel (✉) · A. Schucknecht · J. Matschullat
Interdisciplinary Environmental Research Centre, TU Bergakademie Freiberg, Brennhausgasse 14, 09599 Freiberg, Germany
e-mail: stephanie.haensel@ioez.tu-freiberg.de

Published online: 12 February 2015

1 Introduction

Observed and projected increases in precipitation extremes, such as intense rain, snow, sleet or hail as well as severe dry and wet phases impact many economic sectors (e.g. agriculture, forestry, water management). Related potential effects have recently been extensively discussed (e.g. Easterling et al. 2000; Fink et al. 2004; Lehner et al. 2006; Kundzewicz et al. 2006; Rebetez et al. 2006). Regional-scale analyses and consequently societal adaptation to the inevitable consequences of changing local and regional climatological conditions are needed since effects of global climate change vary notably on spatial scales.

We study observed and projected monthly precipitation data for the greater Dresden area in Saxony, Germany. Recent examples for the vulnerability of the study region to extreme events are the major Central European flood event in August 2002 (Ulbrich et al. 2003), the Europe-wide heat wave and drought in the summer of 2003 (Fink et al. 2004; Schönwiese et al. 2004) and the Elbe flood in June/July 2013. Future increases in frequency or magnitude of such extreme events would translate into a situation that is not only critical to the economy and for disaster preparedness but would also impact water resources, agriculture and numerous infrastructures. Using an ensemble of 12 RCMs from the ENSEMBLES-project, Schwarzak et al. (2014) described increases in dry spell duration, particularly during summer, more persistent wet spells during winter and increases in the frequency of heavy precipitation events in most seasons and for the late twenty-first century in the study area. Despite projected decreasing average summer precipitation, the most extreme precipitation events above the 99th percentile are likely to increase by the end of the twenty-first century in most seasons. The authors have also shown high biases of some RCMs in the study area, most of them with strong

overestimations of rainfall amounts, thus complicating the evaluation of future drought severity (Schwarzak et al. 2014).

Several indices are in practical use to identify and assess frequency, duration and intensity of extreme precipitation events on different timescales (e.g. index lists by Karl et al. 1999; Manton et al. 2001; Nicholls and Murray 1999). Heavy precipitation events as well as dry and wet periods are often analysed based on indices of daily precipitation totals; but long-term drought events and wet periods leading to serious water shortage in the water sector, are best assessed based on monthly and seasonal precipitation totals. Drought indices like the Standardised Precipitation Index (SPI) (McKee et al. 1993) are applied for that purpose.

The study of standardised precipitation anomalies as applied here, allows for the comparison of models with different biases (related to observation data). Here, two precipitation anomaly indices were selected. The first is the internationally widely accepted SPI (McKee et al. 1993) which has been proposed as the universal drought index by the WMO (*Lincoln Declaration on Drought Indices*, WMO 2009; Hayes et al. 2011). The second one is the computationally less demanding Rainfall Anomaly Index (RAI; van Rooy 1965) in its modified version (mRAI). Both indices normalise precipitation data, albeit with a more complex procedure for the SPI. While the SPI is widely used internationally (Guttman 1999; Wu et al. 2007; Moreira et al. 2013; Zhang et al. 2013), including the analysis of projection results (Heinrich and Gobiet 2012; Vidal et al. 2012), the RAI receives a lot less attention (Tilahun 2006). Nevertheless, several studies have already shown a comparable performance to the SPI (Keyantash and Dracup 2002; Loukas et al. 2003). The RAI offers a higher degree of transparency and tractability and demands a lower degree of sophistication than the SPI with regard to the evaluation criteria for drought indices as proposed by Keyantash and Dracup (2002). In principle, the RAI may be calculated on the same timescales as the SPI and is similarly robust. Here, we focus on shorter timescales of 1 to 6 months.

This study assesses if the mRAI delivers equivalent results to the SPI and may thus be used as a computationally less demanding alternative to the SPI in evaluating future extreme precipitation characteristics on monthly to seasonal scales. Generally, projections derived from climate models come with manifold uncertainties. These uncertainties relate to, e.g. the future development of the human society—represented by greenhouse gas emission scenarios, the variability of results due to the selection of a climate model (which uses different schemes of simplifying the complex climate system) and last but not least, to the internal climate variability—represented by different runs of the same climate model. Multi-model ensemble approaches are used to increase the confidence in the projected future climate changes in order to build a robust basis for mitigation and adaptation decisions.

We address the question, if the differences between the two indices SPI and mRAI influence the interpretation of the climate model ensemble results. The exemplary analysis is based on a total of twelve runs from five regional climate models (RCMs) for the study area. The focus was set on the comparison of the results that both indices delivered and not on the individual RCMs used in this study or the specific ensemble results for the study area.

2 Materials and methods

2.1 Study area

The greater Dresden area in Saxony, Germany (model region of the climate adaptation project REGKLAM; see www.regklam.de) was selected as a representative region for the temperate climate zone of Central Eastern Europe (Fig. 1). The region features a warm temperate, fully humid climate with warm summers (Koeppen climate classification: Cfb climate; Kottek et al. 2006). The annual mean temperature was 8.3 °C, and the annual mean precipitation was 793 mm during the climate normal 1961–1990. Climate differences in the study area are mainly related to the influence of the mid-elevation mountain ranges to the south (Erzgebirge). While the mean temperature is primarily linked to altitude (mean annual temperature of 9 °C in Dresden-Klotzsche, 222 m a.s.l., versus 4.5 °C in Zinnwald, 877 m a.s.l.), the precipitation distribution (mean annual precipitation of 640 mm in the lowlands and of 1000 mm on the mountain ridges) is additionally affected by the position of the mountains in relation to the prevailing wind direction (Bernhofer et al. 2009).

2.2 Data

The comparison of dry and wet anomalies between mRAI and SPI was based upon 20 rain gauge stations (Fig. 1) for the observation period 1951–2010 and on the output of an ensemble of five RCMs, reflecting two dynamical and three statistical downscaling approaches for the period 1961–2100. All of these RCMs were nested within the global climate model ECHAM5/MPI-OMT63L31 (Roeckner et al. 2003, 2004, 2006). We used precipitation simulations of the two physical dynamical downscaling techniques REMO (Jacob and Podzun 1997; Jacob et al. 2008) and COSMO-CLM (Hollweg et al. 2008). The three statistical RCMs involved different versions of the same weather pattern-based downscaling method, developed by CEC Potsdam (http://www.cec-potsdam.de/Produkte/Klima/WettReg/wettreg.html); WEREX IV (Enke et al. 2001, 2005), WETTREG 2006 (Spekat et al. 2007) and WETTREG 2010 (Kreienkamp et al. 2010a, b). The physical models provide grid data with different spatial resolutions, while the statistical models

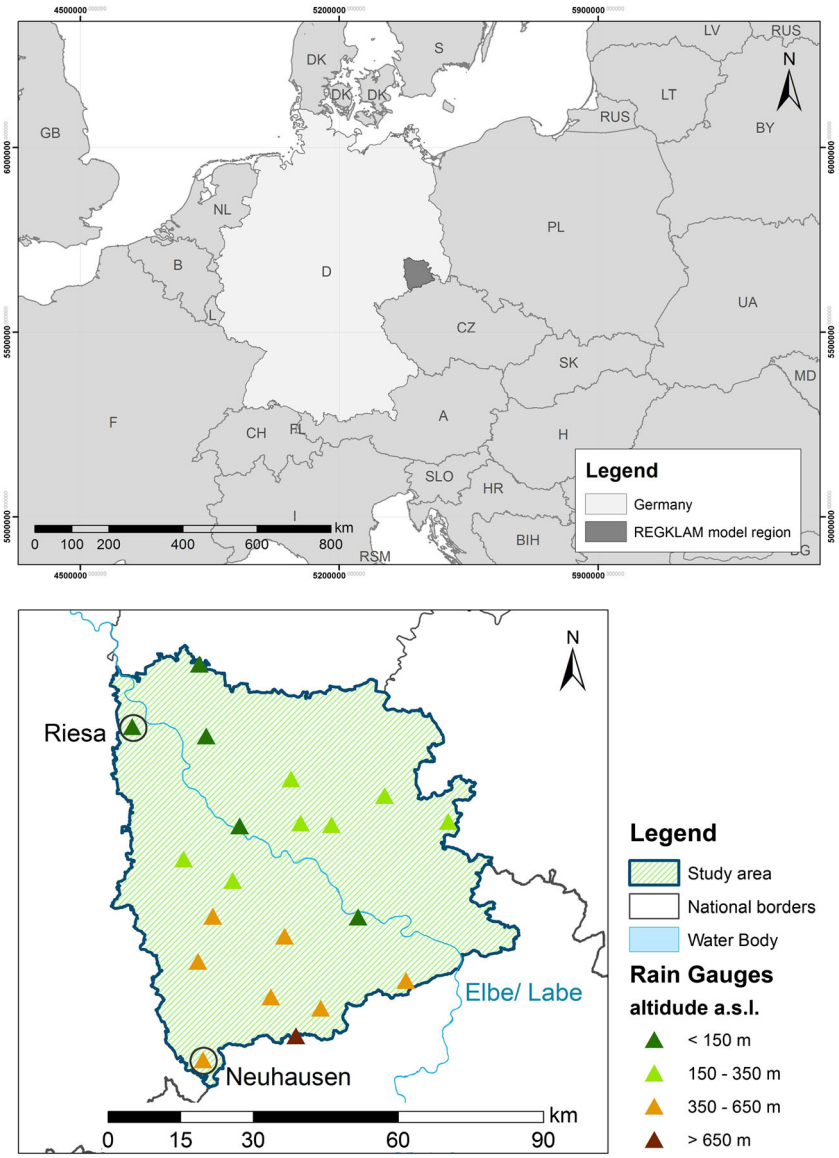

Fig. 1 Location of the study area within Europe (*upper panel*) and location of the rain gauge stations within the study area (*lower panel*)

provide data as point information (stations correspond to observation data).

We solely focussed on the emission scenario A1B (Nakicenovic and Swart 2001), since analyses of the five REGKLAM-RCMs have shown much larger variability in projected precipitation of the different models as compared with the different emission scenarios (Bernhofer et al. 2011). The number of individual runs differs between the RCMs, with a larger number for the statistical ones. The physical RCMs are a lot more complex in their calculation requirements and need much longer computing times. Of these RCMs, only one run (REMO) and two runs (CLM) were available for the REGKLAM project. Ten realisations were available for each of the statistical models, yet we display only three results that have been synthesised from the ten realisations. These runs are called normal, dry and wet for WEREX IV and WETTREG 2006; indicating their general precipitation characteristics over the entire study period 1961–2100 (Spekat et al. 2007). For WETTREG 2010, the arithmetic average of all ten runs (Avg.), the run delivering the lowest (Min.) and the highest (Max.) value or trend, were used (Table 3). Detailed information about these climate projections can be obtained from Bernhofer et al. (2011) and references therein.

2.3 Precipitation anomaly indices

The Standardised Precipitation Index (SPI), developed by McKee et al. (1993), is based on the probability distribution of precipitation. The calculation is made by fitting a

probability distribution function to a long-term precipitation series, which is then transformed into a normal distribution. The SPI can be calculated for different timescales. For a detailed information about the general calculation of the SPI, see McKee (1993, 1995) and Guttmann (1998, 1999). In this study, the SPI is calculated for the timescales of 1 month (SPI-1), 3 months (SPI-3), 6 months (SPI-6) and 12 months (SPI-12), fitting a gamma probability density function to the monthly precipitation record of the period 1961–2000.

The Rainfall Anomaly Index (RAI), designed by van Rooy (1965), considers the rank of the precipitation values to calculate positive and negative precipitation anomalies. The original calculation of the RAI was modified to better fit the 40-year-long validation period 1961–2000 and to achieve a maximum comparability to the SPI. The modified RAI—mRAI—of a certain month i is calculated in this study as follows:

$$\mathrm{mRAI}_i = \pm SF \cdot \left(P_i - \overline{P}\right) / \left(\bar{E} - \overline{P}\right), \quad (1)$$

where

P_i	Monthly precipitation sum of month i
$\overline{P}$	Median monthly precipitation of the validation period 1961–2000 for the respective month (e.g. if i is January, then $\overline{P}$ is the median of all January precipitation sums of the years 1961–2000)
$\bar{E}$	Mean of the 10 % most extreme precipitation sums (10 % percentile for positive anomalies, 90 % percentile for negative anomalies) of the validation period 1961–2000 for the respective month (e.g. if i is January, then $\bar{E}$ is the mean of the 10 % most extreme January precipitation sums of the years 1961–2000)
$\pm SF$	Scaling factor (positive for $P_i \geq \overline{P}$, and negative for $P_i < \overline{P}$)

We use the median instead of the arithmetic average to estimate the mean of the precipitation time series $\overline{P}$ for 1961–2000, as the precipitation distributions are skewed at most of the analysed timescales. $\bar{E}$ represents the mean of the four most extreme events of the validation period 1961–2000 in our RAI calculation. Originally, $\bar{E}$ was used to characterise the variability of the dataset and referred to the ten most extreme events (van Rooy 1965). We modified the amount of extreme events in the calculation of $\bar{E}$, as our underlying time period is notably shorter than the ones van Rooy (1965) used in his analysis. We believe that considering the 10 % highest and lowest values, respectively, delivers more realistic results and furthermore refers to the general definition of moderate extreme events. Applying different values of $\bar{E}$ for the positive and negative precipitation anomalies is a simple mechanism of accounting for the asymmetry of distributions and is preferred over the use of the standard deviation. Originally, van Rooy (1965) used a scaling factor of SF=3. We apply an SF=1.7, thus aiming at similar values and class frequencies as those of the SPI. For other climate regions and applications the scaling factor may be adjusted.

The mRAI can also be calculated on timescales exceeding 1 month, similar to the SPI. The same timescales (1 month (mRAI-1), 3 (mRAI-3), 6 months (mRAI-6) and 12 months (mRAI-12)) were calculated for the comparison with the SPI. The main focus was on the monthly timescale, yet seasonal and yearly anomalies were compared, too.

The dimensionless mRAI and SPI values can be evaluated according to a classification scheme. We modified the original classification of van Rooy (1965) and McKee (1993) in order to: 1) develop SPI classes for wet conditions, 2) include a 'near normal' condition class and 3) create a classification for mRAI and SPI that results in comparable frequencies. The original classifications and our modified classification with nine classes ranging from extremely wet to normal to extremely dry are shown in Table 1.

Table 1 SPI and RAI classification according to their original definitions and a modified definition as applied in this study

Original definition (McKee et al. 1993)		Original definition (van Rooy 1965)		Classification used in this study		
SPI	Description	RAI	Description	Class	SPI and mRAI	Description
		≥3.00	Extremely wet	1	≥2.00	Extremely wet
		2.00 to 2.99	Very wet	2	1.50 to 1.99	Very wet
		1.00 to 1.99	Moderately wet	3	1.00 to 1.49	Moderately wet
		0.50 to 0.99	Slightly wet	4	0.50 to 0.99	Slightly wet
		−0.49 to 0.49	Near normal	5	−0.49 to 0.49	Near normal
0.00 to −0.99	Mild drought	−0.99 to −0.50	Slightly dry	6	−0.99 to −0.50	Slightly dry
−1.00 to −1.49	Moderate drought	−1.99 to −1.00	Moderately dry	7	−1.49 to −1.00	Moderately dry
−1.50 to −1.99	Severe drought	−2.99 to −2.00	Very dry	8	−1.99 to −1.50	Very dry
≤−2.00	Extreme drought	≤−3.00	Extremely dry	9	≤−2.00	Extremely dry

2.4 Comparison of both indices

Both indices were calculated and compared for the period 1951–2010 (measured precipitation data; observations) and for the period 1961–2100 (RCM data). Selected rain gauge station data were compared for the observation period and are displayed to show how regional differences such as altitude may influence the comparability of both indices. In addition, averaged index values over the study areas were compared to ensure the comparability with the display of the RCM data. For the RCM data, only index values and trends, averaged over the study area, were compared to ease the display and interpretation of the RCM ensemble results. Thereby, the precipitation anomaly indices were initially calculated separately for each data point (raster cell or station) that covers a part of or is situated within the study area. The individual signals were averaged thereafter. Directly calculating the anomaly indices for the regionally averaged precipitation is not suitable, as the spatial averaging of the precipitation would strongly smooth the precipitation distribution; thus rendering a realistic representation of precipitation extremes impossible.

The analyses cover the study period 1951–2100 with a focus on the validation period 1961–2000 and the time-slice comparisons of 2021–2050 and 2071–2100 versus the last climate normal 1961–1990. The correlation between the indices SPI and mRAI was evaluated for the observations for 1951–2010, using the Pearson product moment correlation coefficient und the Spearman rank correlation coefficient. *X*-*Y* scatterplots were used to illustrate the relationship between the two indices on a monthly scale. Pearson correlation coefficients were evaluated for the RCM monthly index values for two periods, namely 1961–2000 and 2061–2100 (Table 3). In addition to the *X*-*Y* scatterplots, time series of the 2 months with the lowest and the highest correlation of both indices are displayed in Fig. 3 for the regional average of the observations and in Fig. 6 for the RCMs. Two selected observation stations (Fig. 1), representing the lowlands and the mountainous areas of the study area, were chosen to evaluate spatial influences on the index comparison. These monitoring stations are located near Riesa in the northern lowlands of the study area (142 m a.s.l.) and Neuhausen in the southern Erzgebirge (593 m a.s.l.).

The frequencies of SPI and mRAI in the nine anomaly classes (Table 1) were compared for the observations of all months (Fig. 4) and for the RCMs of January and July (Fig. 5) within the validation period 1961–2000. Precipitation anomalies were standardised to the validation period 1961–2000, resulting in a mean precipitation anomaly of zero for this period for all RCMs. Thus, individual RCM biases to observed precipitation data are irrelevant for the subsequent analyses. Existing RCM biases are not displayed here.

Linear trends and Mann–Kendall trends (Mann 1945; Kendall 1970) of the index series were calculated for 1951–2000 (observations; Fig. 3) and for 2001–2100 (RCM data; Fig. 6; Table 6). Changes in the frequency distribution of the indices were analysed by comparing the time slices 2021–2050 (mid-twenty-first century) and 2071–2100 (late twenty-first century) with the reference period 1961–1990. These analyses were done for the months (Fig. 7; Table 5), the seasons (Fig. 8; Table 4) and the half years (summer half year (SHY)—AMJJAS; winter half year (WHY)—ONDJFM; Fig. 9; Table 4). The focus was laid on the classes representing ‘very dry/wet’ and ‘extremely dry/wet’ conditions.

3 Results and discussion

3.1 Observation data

Correlations The correlations between the index time series, averaged over the study area (timescale, 1 month), are displayed in Fig. 2 for all months. SPI and mRAI are highly correlated, with all Pearson product moment correlation coefficients above 0.959. More than 90 % of the variability of the SPI is explained by the mRAI. While a linear model may approximate the relation between both indices, it is not completely linear. There is a tendency for lower SPI than mRAI values—particularly in the range of extreme conditions (index values, >2 and ≤-2, respectively), while the mRAI tends to have slightly lower values in the normal range. Accordingly, the correlations are even higher if applying the Spearman rank correlation coefficient (0.997 to 1.000).

The comparatively low Pearson correlation coefficients in April (0.962) and September (0.959) are due to exceptionally low SPI values of −5.0 (April 2007) and −4.6 (September 1960), respectively. These values are connected with monthly precipitation totals of 0.8 and 1.0 mm averaged over the study area and several zero precipitation values at station level. The SPI reacts very sensitive to such low precipitation totals and may yield unrealistically low values as already described by Hayes et al. (1999) and Lloyd-Hughes and Saunders (2002). The associated mRAI values are only about half as large, but they still belong to the class of ‘extreme drought’. This lower sensitivity of the mRAI in depicting the magnitude of dry extremes must not be a disadvantage or limitation, as in most times the class of ‘extreme drought’ is reached and the absolute magnitude of the index is not to be interpreted.

Figure 3 shows the time series’ similarity of both indices (timescale, 1 month) and related linear trends for the observation data, averaged over the study area, and additionally for two exemplary months at two representative rain gauge stations (Riesa and Neuhausen). These months were selected according to the correlation coefficients over the study area. The lowest Pearson correlation occurred in September (0.959) and the highest Spearman correlation in October (1.000). The

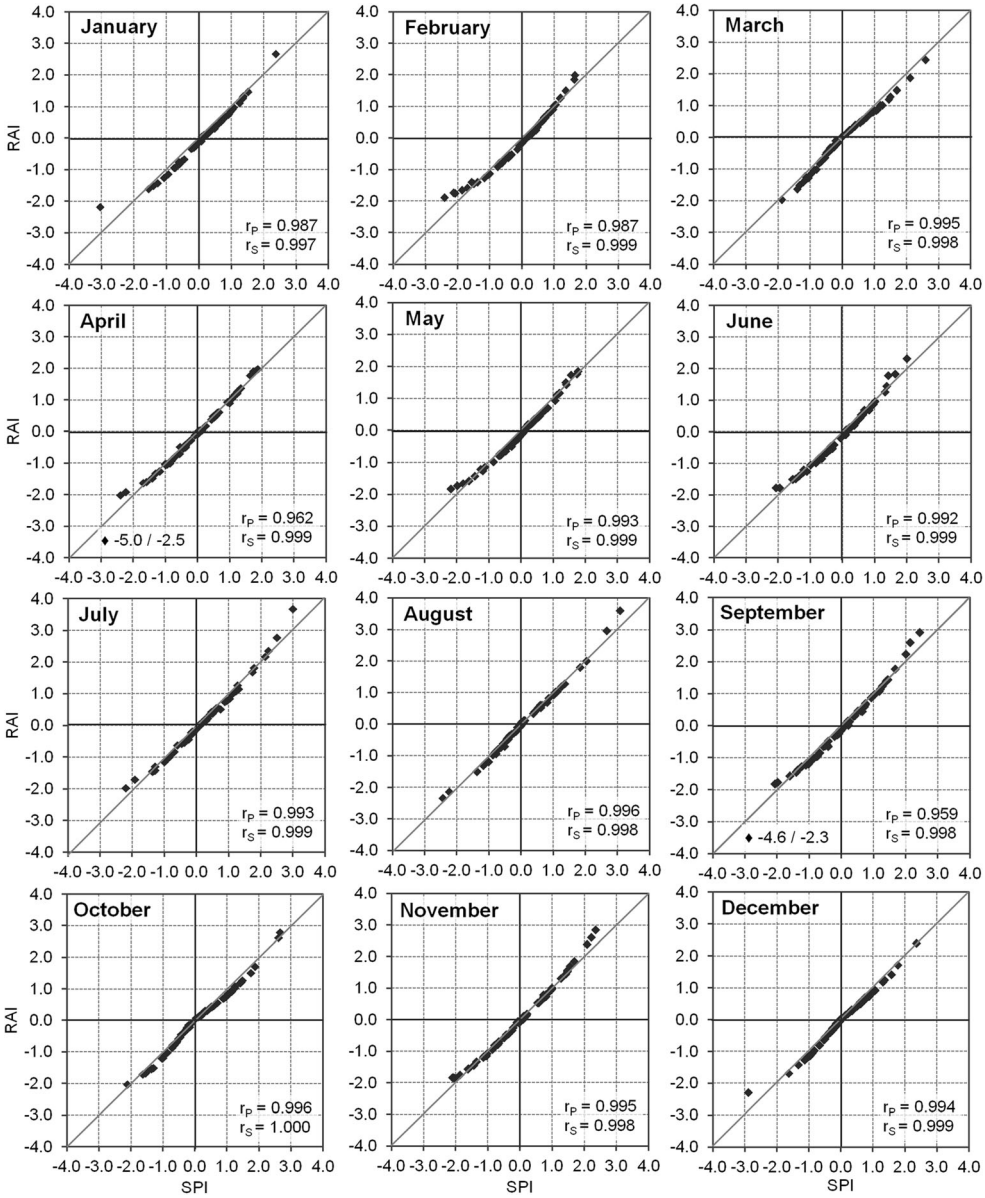

Fig. 2 Correlation between SPI-1 and mRAI-1 within 1951–2010 for all months; values averaged over the REGKLAM-model region

correlation coefficients of the station data are in a similar range as those of the study area average displayed in Fig. 2. The Pearson correlation coefficients of both index time series for the period 1951–2010 range for all months from 0.933 (September) to 0.997 (August) at Riesa and from 0.938 (September) to 0.998 (November) at Neuhausen. The Spearman correlations are 1.000 for almost all months for both stations. The course of the SPI and the mRAI time-series curves is very similar for the station data as well as for the regional average. Considerable deviations occur only for the most extreme dry events, e.g. September 1960. The correlation analyses show that the mRAI fits the SPI very well, even for the highly skewed monthly precipitation totals.

Trends Generally, the computed linear trends are very much the same for both indices and the regional differences in the trends are larger than the differences between the two indices (Fig. 3; Table 2). Opposite trend directions may be indicated by the SPI and the mRAI only if the change signals in the time series are very small. These differences are not relevant, however, as they occur only for time series without significant changes. The significance of the monthly precipitation anomaly trends for 1951–2000 using the Mann–Kendall trend test is shown for 18 stations within the study area and for the average over the entire region in Table 2 (trends for two stations with shorter times series are not indicated). The Mann–Kendall trend delivers almost identical values and related statistical significances for both indices. This is true for the individual stations and for the regional average in all months. No general statistically significant monthly precipitation trend emerged for the period 1951–2000 in the study area. Only November showed some indication of increasing precipitation totals at

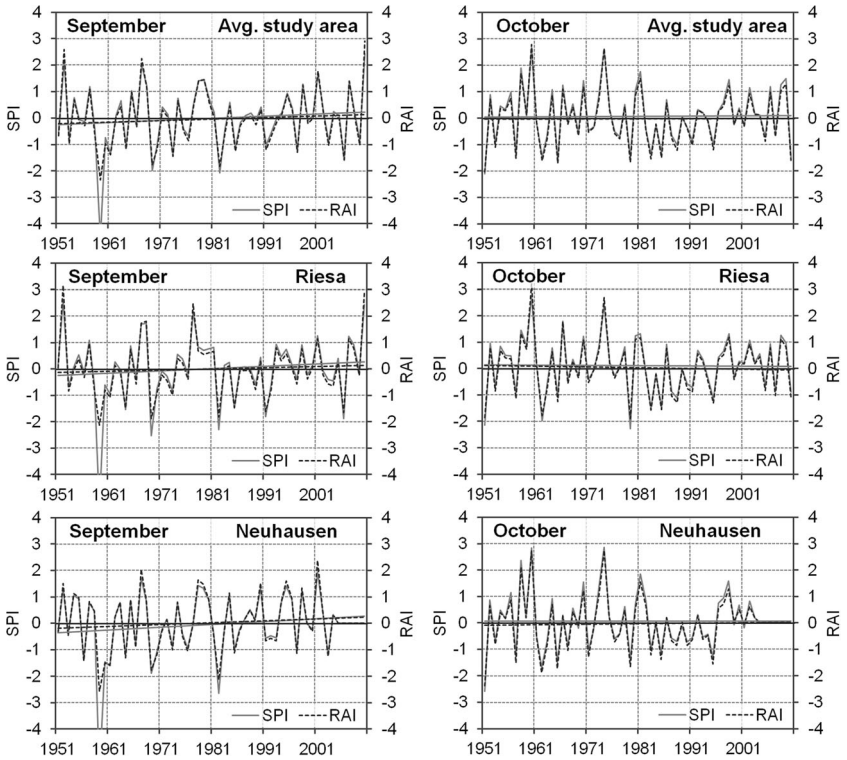

Fig. 3 Comparison of SPI-1 and mRAI-1 time series and related linear trends for September and October (1951–2010) averaged over the study area and at the rain gauge stations Riesa and Neuhausen

more than half of the stations, albeit at a low significance level (α=0.2).

Frequency distribution A comparison between the frequency distribution of the SPI and of the mRAI was made for the period 1961–2000, which was also used as the validation period for the RCMs. The Kolmogorov-Smirnov test showed no significant differences in the distributions of SPI and mRAI. The frequencies within the nine wetness and dryness classes, as depicted in Table 1 and averaged over the study area, are shown in Fig. 4. Similar results were obtained for individual stations (not shown here). The frequency distribution of mRAI classes is not fully symmetrical, yet the statistical tests did not show any significant deviation from the normal distribution at the 5 % significance level. The mRAI shows a slightly higher frequency in the classes 'moderately' and 'very dry' than the SPI, while the mRAI yields fewer events in the 'extremely dry' class. SPI and mRAI are well comparable in their frequencies in the 'extremely' and 'very wet' classes, but the frequency of mRAI in the classes of 'slightly' to 'moderately wet' conditions is lower than the one of SPI in many cases. These (non-significant) deviations in the distributions are caused by the right-skewed distribution of monthly precipitation totals, where the more complex normalisation procedure of the SPI has some advantages over the more simple RAI calculation. In a next step, we are going to assess if these deviations in the frequencies of individual moisture condition classes are significantly skewing the results of a regional climate model ensemble.

3.2 Regional climate models

RCM validation The regional models were validated against the observation dataset for the period 1961–2000 by comparing the frequency distribution of each RCM run with the observed characteristics (Fig. 5; exemplary for January and July). All model runs reflect the general frequency distribution of the anomaly classes rather well—despite differences in absolute precipitation deviations (Bernhofer et al. 2011). Individual model runs partly show a large range in the percentage of certain precipitation anomaly classes; this is most distinct for the 'near normal' class. The general characteristics of individual models are preserved by the mRAI and SPI. For instance, the dry run of WEREX IV shows a lower percentage in the 'near normal' class for both indices and a higher percentage in the 'slightly dry' class for January as compared to the observation data. The general 'overestimation' of the frequency in the classes moderately and very dry by the mRAI and the 'underestimation' in the classes 'slighly' and 'moderately wet' is also visible in the RCM ensemble.

Correlations The linear Pearson product moment correlation coefficients between the precipitation indices SPI and mRAI for monthly time series, averaged over the study area, are similarly large for the model runs (Table 3) as already shown for the observations (Fig. 2). They range between 0.929 and 1.000, with most values above 0.990. The only exceptions are the values of the minimum and maximum run of WETTREG 2010 that show consistently lower correlations, yet most

Table 2 Mann–Kendall trends for the two precipitation anomaly indices SPI and RAI, calculated for 18 rain gauge stations and using the regional average of the study area for 1951–2000

		Riesa	Großenhain-Skassa	Gröditz	Pulsnitz	Bischofswerda	Radeburg	Langebrück	Tanneberg	Grumbach	Dippoldiswalde	Pirna	Coswig	Tharandt-Grillenburg	Oberbobritzsch	Lauenstein	Neuhausen (Erzgebirge)	Altenberg-Kipsdorf	Rosenthal-Bielatal	Average over tge study area
Jan	**SPI**	-0.10	0.17	-0.48	0.74	0.04	-0.24	0.66	-0.95	-0.13	-0.64	-0.18	-0.38	0.99	-0.32	0.13	-0.53	-0.12	-0.63	0.01
	RAI	-0.09	0.16	-0.47	0.74	0.03	-0.23	0.67	-0.95	-0.09	-0.64	-0.17	-0.37	0.99	-0.33	0.12	-0.54	-0.12	-0.61	-0.03
Feb	**SPI**	0.08	0.49	0.78	0.28	1.03	0.85	0.96	0.53	1.32	0.98	1.18	0.61	1.16	0.44	1.08	0.43	0.54	0.92	0.83
	RAI	0.08	0.51	0.80	0.28	1.03	0.86	0.95	0.57	1.31	0.95	1.17	0.60	1.15	0.46	1.09	0.43	0.53	0.92	0.81
Mar	**SPI**	-0.04	0.20	0.57	0.39	1.18	0.11	0.31	0.00	0.27	0.09	-0.13	-0.19	0.60	0.97	0.58	1.17	0.76	0.28	0.34
	RAI	-0.06	0.20	0.55	0.38	1.17	0.12	0.31	0.01	0.25	0.10	-0.11	-0.21	0.61	0.95	0.59	1.18	0.74	0.27	0.38
Apr	**SPI**	-0.79	-0.80	-1.03	-0.60	-0.69	-0.61	-0.16	-1.23	-0.47	-0.58	-1.41	-0.58	-1.19	-1.22	-0.38	-0.35	-0.77	-2.01	-0.79
	RAI	-0.79	-0.82	-1.03	-0.60	-0.69	-0.61	-0.12	-1.23	-0.48	-0.60	-1.39	-0.58	-1.19	-1.21	-0.36	-0.37	-0.38	-2.00	-0.83
May	**SPI**	-1.11	0.24	-0.98	0.17	-0.22	-0.09	-0.53	-0.95	-0.28	-0.28	-0.01	-0.39	0.08	-0.27	-0.84	-0.17	-0.47	-1.12	-0.29
	RAI	-1.10	0.25	-0.97	0.17	-0.23	-0.11	-0.52	-0.95	-0.28	-0.28	-0.01	-0.40	0.06	-0.26	-0.84	-0.18	-0.49	-1.12	-0.26
Jun	**SPI**	-1.02	-1.15	-1.21	-0.66	-0.67	-0.32	-0.41	-1.70	-1.29	-0.94	-0.04	-1.38	-1.26	-0.74	-0.16	1.05	-0.49	0.13	-0.83
	RAI	-1.02	-1.14	-1.22	-0.65	-0.67	-0.34	-0.40	-1.71	-1.30	-0.94	-0.02	-1.38	-1.24	-0.75	-0.17	1.05	-0.50	0.10	-0.63
Jul	**SPI**	-0.81	-0.82	-1.19	-0.88	-1.12	-0.43	-0.49	-0.02	0.31	-0.55	-0.64	-0.27	0.37	0.04	-0.14	0.13	-0.38	-0.42	-0.44
	RAI	-0.81	-0.82	-1.20	-0.84	-1.11	-0.43	-0.49	-0.03	0.30	-0.55	-0.63	-0.25	0.39	0.04	-0.14	0.11	-0.38	-0.40	-0.48
Aug	**SPI**	-0.52	0.01	-0.68	1.25	0.19	-0.28	0.76	0.35	0.39	0.34	0.29	-0.13	0.61	0.04	0.70	1.40	1.53	0.32	0.24
	RAI	-0.49	0.01	-0.67	1.27	0.18	-0.25	0.76	0.35	0.39	0.34	0.31	-0.12	0.60	0.05	0.70	1.40	1.53	0.32	0.39
Sep	**SPI**	0.47	0.28	0.32	0.57	0.29	-0.13	0.38	-0.30	0.50	-0.18	0.38	0.25	-0.05	-0.07	0.78	0.68	0.55	0.41	0.31
	RAI	0.49	0.28	0.31	0.57	0.29	-0.13	0.38	-0.31	0.50	-0.18	0.39	0.26	-0.06	-0.08	0.76	0.66	0.55	0.41	0.33
Oct	**SPI**	-0.59	-0.43	-0.92	0.36	0.14	-0.07	0.31	-0.41	0.31	-0.52	-0.22	-0.32	-0.14	0.28	-0.19	0.26	0.30	-0.55	-0.08
	RAI	-0.59	-0.43	-0.91	0.37	0.17	-0.07	0.30	-0.43	0.31	-0.54	-0.22	-0.33	-0.14	0.27	-0.19	0.26	0.30	-0.53	-0.03
Nov	**SPI**	0.93	0.72	1.05	0.77	1.11	0.88	1.45	2.14	2.13	1.29	1.41	1.48	2.18	1.54	1.62	0.86	1.36	0.71	1.55
	RAI	0.93	0.71	1.05	0.77	1.13	0.87	1.45	2.15	2.16	1.30	1.40	1.50	2.16	1.53	1.61	0.88	1.38	0.70	1.63
Dec	**SPI**	0.10	0.29	0.37	-0.04	0.23	0.27	0.44	0.62	1.25	0.62	0.51	0.35	0.61	0.69	0.84	0.59	0.45	-0.11	0.39
	RAI	0.11	0.28	0.39	-0.04	0.23	0.24	0.45	0.62	1.26	0.64	0.50	0.37	0.62	0.68	0.81	0.59	0.44	-0.09	0.41

The background colour indicates the direction (blue, precipitation increase; orange, precipitation decrease) and the significance of the trends (the darker the colour, the higher the statistical significance)

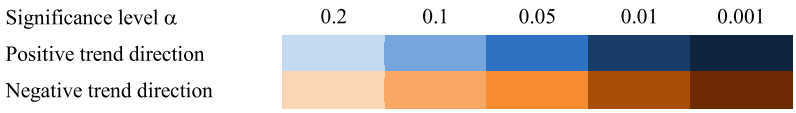

values are still above 0.950. The lower correlations for these two ensemble members are explained by their creation from ten runs of the model WETTREG 2010. The minimum/maximum values may belong to another model run each year and slight differences in the min/max as identified by the two indices add up to a weaker correlation than for the individual runs (correlation coefficients between 0.975 and 1.000). The correlations remain high (>0.97) for the time series of the ensemble mean. The correlations are robust over time—there are no systematic deviations in the magnitude of the correlations between the validation period 1961–2000 and the end of the twenty-first century (2061–2100). This demonstrates that the mRAI does not develop significant systematic deviations to the SPI within a changing climate and may be applied for climate projections.

The monthly time series of the RCM with the lowest and the highest Pearson correlation coefficient are shown exemplarily for the entire study period 1961–2100 in

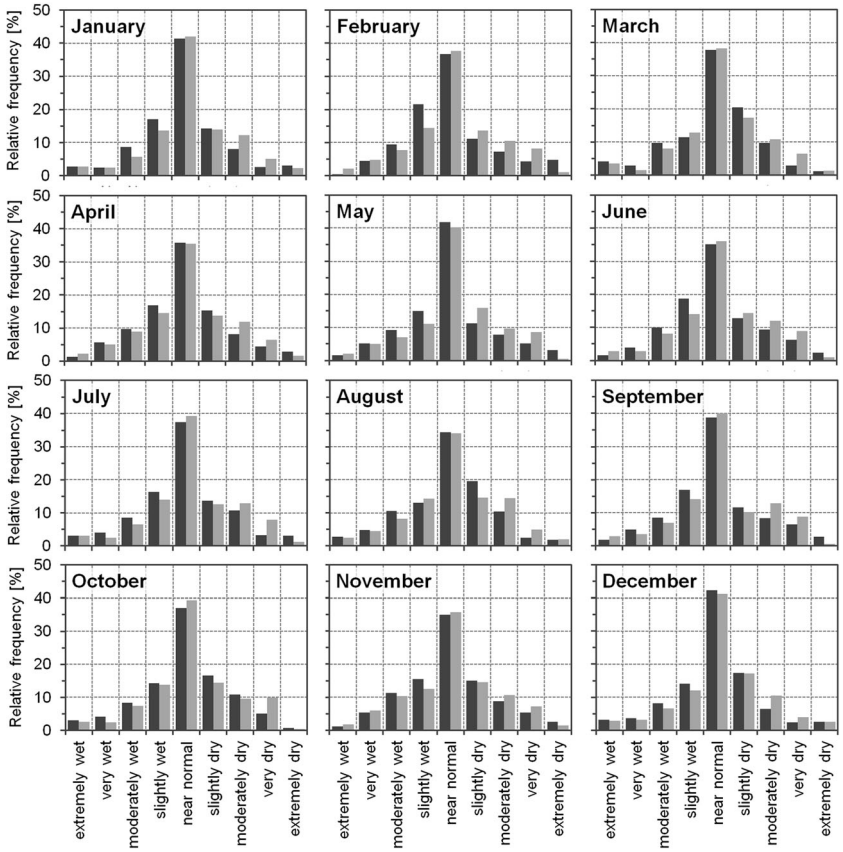

Fig. 4 Frequency distribution of precipitation anomaly classes for observation data from 1961 to 2000. *Dark grey* represents the SPI-1, and *medium grey* represents the mRAI-1

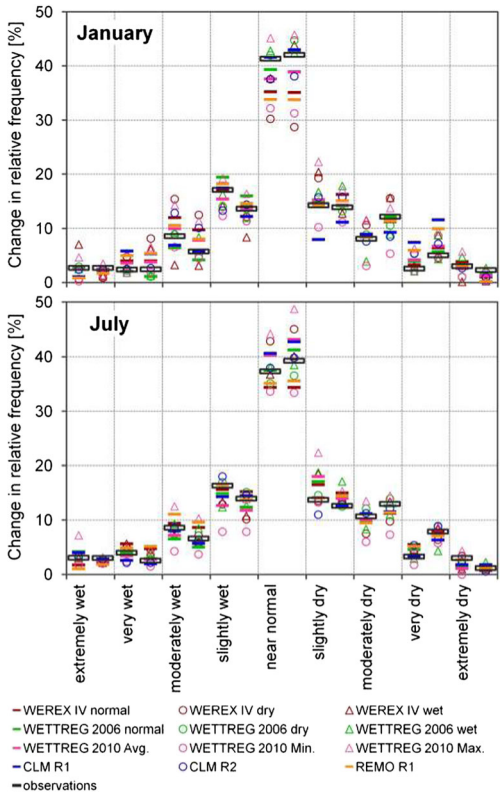

Fig. 5 Frequency distribution of monthly precipitation for January and July, based on the SPI (*left column in each class*) and the mRAI (*right column in each class*), on observation data and on 12 regional climate projections under the SRES scenario A1B averaged over the study area

Fig. 6. Both belong to the model REMO with 0.937 (March, 2061–2100) and 1.000 (June, 1961–2000). Lower than usual correlations are mainly due to higher mRAI than SPI values for the dry and wet extremes. The absolute mRAI and SPI values of extreme events are to be interpreted with great care, but the influence of these deviations between the two precipitation anomaly indices on the evaluation of changes in the frequency of extreme events are comparatively low as shown in Figs. 7, 8 and 9 and in Tables 4 and 5.

Change in the mean and statistical significance The absolute seasonal change signals of mRAI and SPI for the late twenty-first century (2071–2100 compared with 1961–1990) are given in Table 4 for each of the 12 ensemble members. The trends for the mid-twenty-first century are not shown here since they are comparatively small with a large bandwidth of individual RCM results. Generally, the relative magnitude of the change signals is well comparable between mRAI and SPI. The RCMs based on dynamical downscaling approaches (CLM and REMO) show an increase in the mean precipitation anomaly indices in spring (related to wetter conditions compared to the reference period). All other RCM runs are characterised by no or negative changes in the spring precipitation anomaly indices. For the summers, more dry episodes as compared

Table 3 Monthly Pearson product moment correlation coefficients between SPI-1 and RAI-1 for 12 RCM-runs (WEREX IV (WX), WETTREG 2010 (WG06), WETTREG 2010 (WG10)) and the ensemble mean (A1B-Avg) averaged over the study area for the two periods 1961–2000 and 2061–2100

		CLM-R1*	CLM-R2*	REMO-R1*	WX-nor	WX-dry	WX-wet	WG06-nor	WG06-dry	WG06-wet	WG10-Avg	WG10-Min	WG10-Max	A1B-Avg
Jan	1961-2000	0.993	0.998	0.994	0.991	0.997	0.988	0.995	0.997	0.984	0.993	0.944	0.972	0.994
	2061-2100	0.998	0.994	0.999	0.986	0.999	0.982	0.998	0.993	0.990	0.994	0.963	0.960	0.995
Feb	1961-2000	0.996	0.994	0.996	0.995	0.984	0.996	0.999	0.997	0.996	0.996	0.960	0.984	0.995
	2061-2100	0.995	0.994	0.993	0.997	0.993	0.992	0.999	0.998	0.996	0.997	0.989	0.990	0.995
Mar	1961-2000	0.986	0.997	0.970	0.999	0.999	0.999	0.983	0.995	0.995	0.999	0.990	0.982	0.987
	2061-2100	0.997	0.998	0.937	0.999	0.998	0.972	0.988	0.983	0.991	0.991	0.987	0.980	0.974
Apr	1961-2000	0.967	0.996	0.988	0.998	0.996	0.990	0.999	0.990	0.999	0.998	0.979	0.970	0.990
	2061-2100	0.984	0.991	0.998	0.996	0.999	0.996	0.999	0.992	0.999	0.994	0.973	0.976	0.983
May	1961-2000	0.999	0.993	0.999	0.988	0.998	0.999	0.999	0.994	0.971	0.998	0.984	0.988	0.996
	2061-2100	0.992	0.989	0.998	0.993	0.973	0.999	0.992	0.993	0.988	0.998	0.987	0.991	0.995
Jun	1961-2000	0.998	0.996	1.000	0.991	0.999	0.999	0.998	0.999	0.998	0.997	0.977	0.981	0.999
	2061-2100	0.997	0.960	0.992	0.988	0.998	0.994	0.996	0.995	0.999	0.994	0.952	0.986	0.992
Jul	1961-2000	0.997	0.997	0.998	0.999	0.996	0.999	0.999	0.999	0.999	0.992	0.935	0.974	0.998
	2061-2100	0.995	0.990	0.978	0.991	0.998	0.997	0.998	0.998	0.997	0.993	0.940	0.962	0.987
Aug	1961-2000	0.997	0.996	0.999	0.999	0.999	0.997	0.996	0.999	0.997	0.996	0.977	0.988	0.998
	2061-2100	0.986	0.992	0.989	0.999	0.999	0.997	0.996	0.998	0.998	0.997	0.929	0.993	0.986
Sep	1961-2000	0.998	0.994	0.998	0.998	0.999	0.991	0.995	0.999	0.997	0.997	0.987	0.985	0.997
	2061-2100	0.996	0.994	0.984	0.997	0.999	0.997	0.993	0.997	0.997	0.989	0.985	0.966	0.994
Oct	1961-2000	0.981	0.994	0.972	0.995	0.995	0.993	0.998	0.998	0.994	0.993	0.978	0.960	0.979
	2061-2100	0.984	0.990	0.994	0.994	0.991	0.995	0.997	0.999	0.996	0.989	0.989	0.957	0.988
Nov	1961-2000	0.996	0.991	0.997	0.994	0.998	0.997	0.998	0.984	0.998	0.997	0.991	0.990	0.997
	2061-2100	0.999	0.983	0.996	0.995	0.998	0.997	0.996	0.990	0.995	0.993	0.990	0.984	0.990
Dec	1961-2000	0.998	0.998	0.992	0.999	0.993	0.990	0.994	0.998	0.998	0.998	0.975	0.985	0.995
	2061-2100	0.998	0.999	0.989	0.999	0.995	0.989	0.995	0.997	0.998	0.997	0.968	0.974	0.994

The magnitude of the correlations is illustrated by the grey background color scale from white = lowest correlation to middle grey = highest correlation coefficient

**R* run number of the driving GCM ECHAM5

with 1961–2000 (negative change signal of anomaly indices) are projected by all model runs for the end of the century. Autumns also show predominantly drier conditions. All model runs—except for WETTREG 2010 with negative trends—show no or a positive trend for the anomaly indices in winter (related to unchanged or wetter conditions).

The significance of the monthly trends projected by the RCMs for the twenty-first century (2001–2100) was tested with the Mann–Kendall trend test. Background colours in Table 6 illustrate the trend significance of the regional average. Both indices generally deliver similar trends with a similar statistical significance. There is a tendency for the mRAI to deliver slightly larger and sometimes more significant trends; yet the general picture is very well comparable.

Changes in the extremes Changes in the frequency distribution are of practical interest in extension to those changes in average precipitation conditions. Despite the small shift in the frequency distribution between mRAI and SPI in the period 1961–2000, projected change signals are very similar for both indices on different temporal scales (Figs. 7–9; Tables 4 and 5). SPI and mRAI show comparable bandwidths and a comparable mean (median and arithmetic average) of the different model runs for the change signals in winter (January) and summer (July).

The mean change signals in the precipitation anomaly classes for January are more or less negligible, when comparing the period 2021–2050 with the reference period 1961–1990. July shows a small tendency towards increases in the dry classes for the same period (Fig. 7). The mean change signals

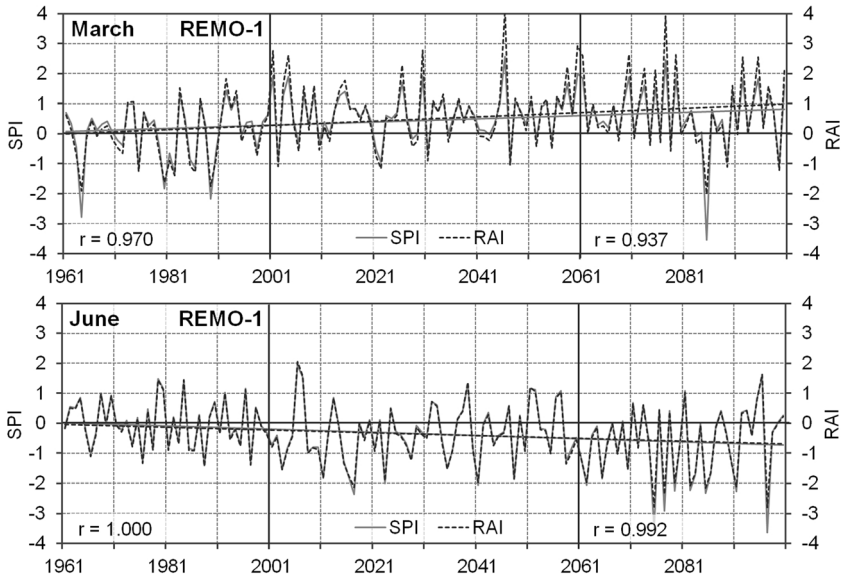

Fig. 6 Time series of SPI-1 and mRAI-1 averaged over the study area for the RCM REMO-R1 under SRES scenario A1B for the months March (*upper panel*) and June (*lower panel*) with linear trends over period 1961–2100 and Pearson correlation coefficients for the sub-intervals 1961–2000 and 2061–2100

of all models remain negligible for January for the late twenty-first century (2071–2100; Fig 7). A clear signal toward more frequent dry conditions is visible for July in period 2071–2100. Moderately to extremely dry conditions became more frequent in almost all regional projections. These changes towards more 'dry extremes' occur during all three summer months (Table 5) and are thus strongly visible in the larger timescales of 3 months (summer; Table 4, Fig. 8) and 6 months (summer half year; Table 4, Fig. 9). Tables 4 and 5 illustrate the seasonal and monthly changes for events above an index value of 1.5 (representing the 'wet extremes') and those below -1.5 (representing dry extremes). The ensemble average shows a plus of 20 % in the frequency of dry extremes in the summer season as well as the summer half year. The frequency within these two classes was 7.0 for the SPI and 8.3 for the mRAI (values averaged over the study area and all months) in the reference period 1961–1990. Thus, more than a doubling in severely to extremely dry conditions is to be expected to occur in summer in the study area at the end of the twenty-first century.

While there are some (non-signficant) differences in the frequencies within the nine classes between the SPI and the mRAI, the trends of average and extreme precipitation are barely influenced. Both precipitation anomaly

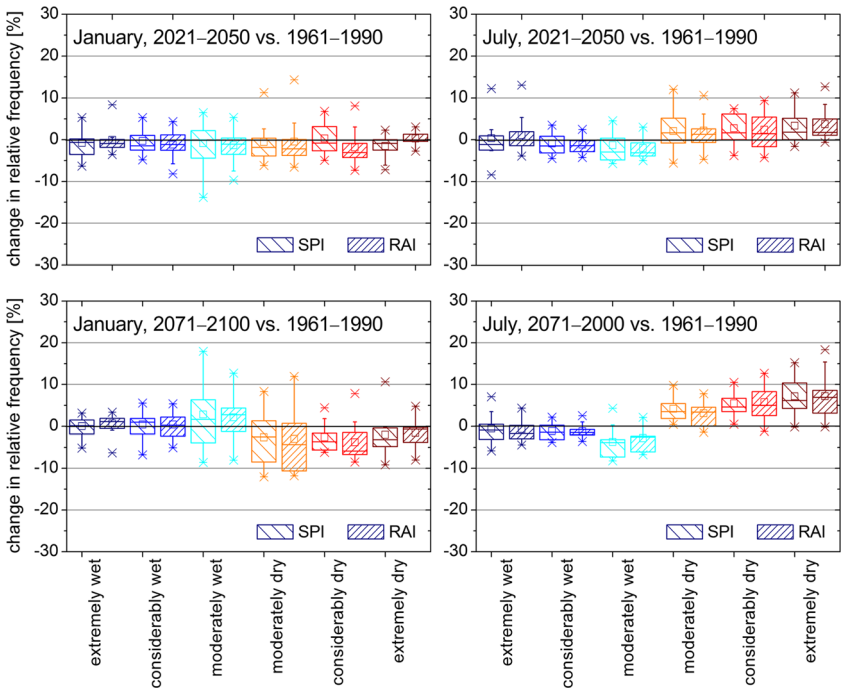

Fig. 7 Changes in the tails of the precipitation distribution averaged over the study area during the months of January (*left*) and July (*right*), based on the SPI and the mRAI on a monthly scale, for an ensemble of 12 regional climate projections under the SRES scenario A1B for the periods 2021–2050 (*upper panels*) and 2071–2100 (*lower panels*) versus period 1961–1990

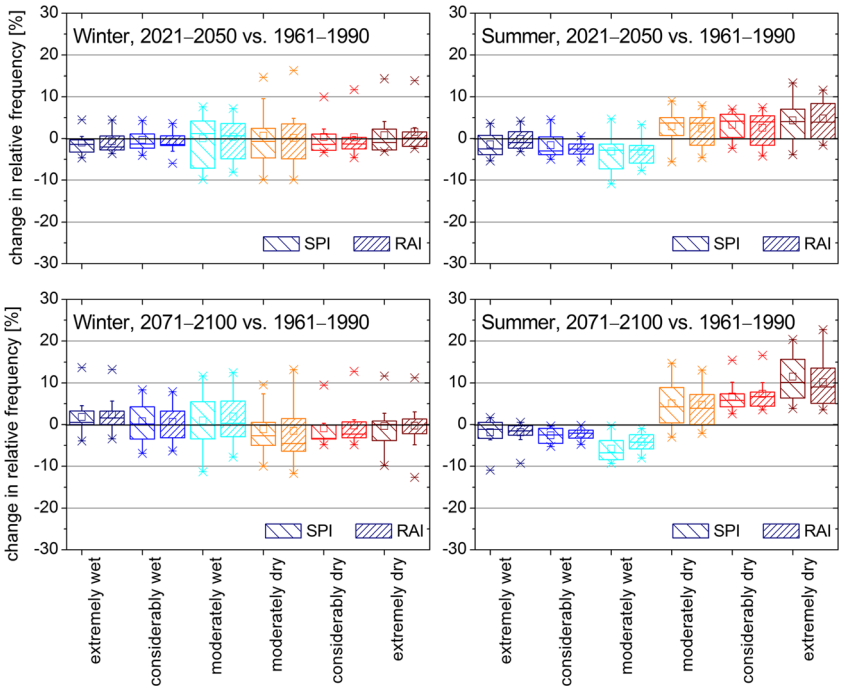

Fig. 8 Same as Fig. 7 but for summer (SPI-3/mRAI-3 for August) and winter (SPI-3/mRAI-3 for February)

indices show a similar range and a similar average of change signals with the clearest overall signal for July for the late twenty-first century period. Thus, the mRAI has shown its applicability as a worthy alternative for the SPI in evaluating the average and extreme precipitation trends of RCM ensembles in the study area, representative for Central Eastern Europe (warm temperate climate zone).

3.3 Adopting the RAI concept for the climatic water balance

Using purely precipitation-based indices such as the SPI and mRAI for the evaluation of future drought conditions may yield underestimations of the drought potential. These indices are only reliable drought estimators, if the other relevant climate parameters behave stationary. This is not the case in a warming climate and with

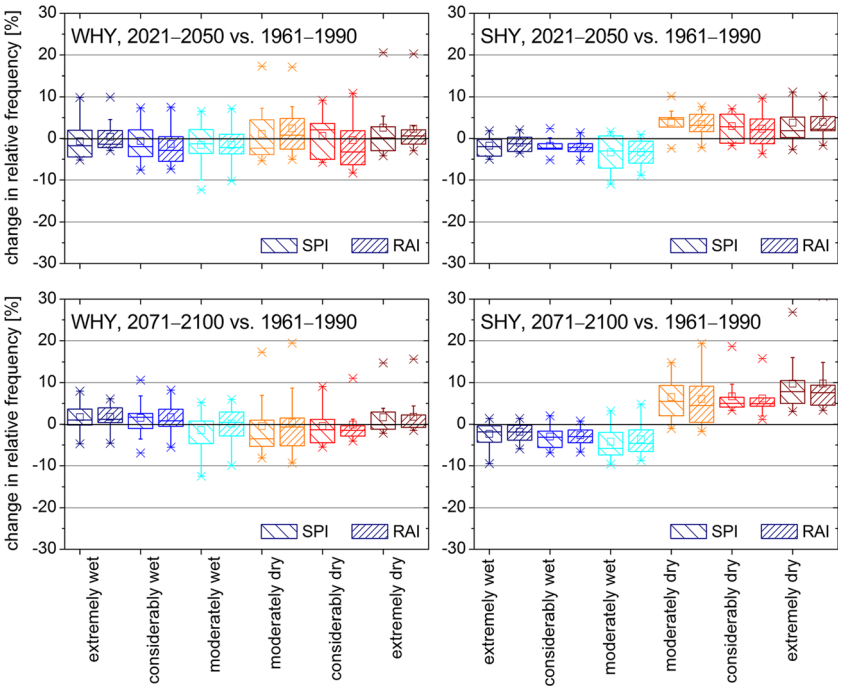

Fig. 9 Same as Fig. 7 but for the summer (SHY, SPI-6/mRAI-6 for September) and winter (WHY, SPI-6/mRAI-6 for March) half years

Table 4 Comparison between the change signals of SPI and mRAI for 2071–2100 versus 1961–1990 for the absolute seasonal precipitation anomalies, the wet extremes and the dry extremes of 12 regional climate projections (WEREX IV (WX), WETTREG 2010 (WG06), WETTREG 2010 (WG10)) and the regional average (A1B-Avg) under SRES scenario A1B

time scale	3-months								6-months			
season	Spring		Summer		Autumn		Winter		SHY		WHY	
index	SPI	RAI	SPI	RAI	SPI	RAI	SPI	RAI	SPI	RAI	SPI	RAI
Change in index averages between 2071–2100 and 1961–1990												
CLM R1	0.61	0.77	-0.70	-0.67	0.08	0.06	0.43	0.43	0.08	0.06	0.43	0.43
CLM R2	0.37	0.35	-0.92	-0.84	-0.25	-0.25	0.55	0.64	-0.25	-0.25	0.55	0.64
REMO R1	0.42	0.44	-0.78	-0.65	0.02	0.02	0.38	0.38	0.02	0.02	0.38	0.38
WX-nor	-0.08	-0.08	-0.91	-0.95	-0.59	-0.54	0.17	0.16	-0.59	-0.54	0.17	0.16
WX-dry	-0.47	-0.46	-0.79	-0.73	-0.39	-0.39	0.10	0.08	-0.39	-0.39	0.10	0.08
WX-wet	-0.23	-0.22	-1.20	-1.18	-0.22	-0.19	0.02	0.01	-0.22	-0.19	0.02	0.01
WG06-nor	-0.11	-0.10	-0.67	-0.63	-0.62	-0.52	0.02	-0.05	-0.62	-0.52	0.02	-0.05
WG06-dry	-0.09	-0.09	-1.06	-1.07	-0.83	-0.77	0.83	0.76	-0.83	-0.77	0.83	0.76
WG06-wet	0.10	0.13	-0.72	-0.67	-0.47	-0.45	-0.04	-0.01	-0.47	-0.45	-0.04	-0.01
WG10-Avg	-0.33	-0.23	-0.56	-0.79	-0.56	-0.28	-0.47	-0.59	-0.51	-0.78	-0.45	-0.51
WG10-Min	-0.64	-0.48	-1.01	-1.33	-0.81	-0.74	-0.77	-0.91	-0.89	-1.39	-0.71	-0.95
WG10-Max	-0.01	-0.05	-0.22	-0.29	-0.20	-0.05	-0.15	-0.31	-0.29	-0.40	-0.24	-0.19
A1B-Avg	0.08	0.10	-0.83	-0.79	-0.28	-0.26	0.13	0.13	-0.28	-0.26	0.13	0.13
Wet extremes: Change in the exceedance frequency of SPI/mRAI > 1.5 [%]												
CLM R1	19.76	19.44	-3.93	-3.46	-5.00	-3.79	5.48	5.82	-4.52	-3.82	5.36	9.57
CLM R2	3.57	3.66	-0.60	-4.63	-3.10	-4.07	13.69	13.85	-4.88	-5.34	5.83	5.72
REMO R1	14.34	13.12	-1.54	-2.07	0.00	-0.31	2.68	2.13	-0.48	-0.70	9.78	8.72
WX-nor	-1.67	-3.62	-5.00	-5.48	-8.50	-7.33	-1.48	-1.64	-2.33	-2.89	-3.49	-2.54
WX-dry	-6.33	-6.29	-7.00	-5.63	-7.33	-6.65	-3.09	-2.80	-6.00	-5.43	-4.90	-6.70
WX-wet	-4.67	-3.68	-7.83	-7.82	-11.83	-9.82	-3.28	-2.33	-1.83	-2.75	-8.05	-8.35
WG06-nor	3.52	2.84	-3.33	-4.02	4.07	4.74	-0.24	-5.15	-6.48	-6.69	1.60	-0.43
WG06-dry	-4.63	-6.63	-8.15	-7.41	-3.89	-3.64	8.56	3.11	-7.78	-6.47	8.52	5.51
WG06-wet	14.81	13.95	-5.37	-2.41	-2.41	-3.64	-1.63	-1.16	-3.33	-1.11	-3.94	-3.30
WG10-Avg	-3.14	-3.17	-6.45	-5.37	-2.15	-2.18	-4.72	-4.68	-6.21	-5.81	-3.95	-4.06
WG10-Min	-7.24	-6.00	-10.19	-7.75	-8.40	-7.13	-6.97	-6.41	-8.46	-8.26	-10.02	-8.56
WG10-Max	0.77	1.60	-2.50	-2.18	7.63	6.43	-1.54	-2.44	1.22	1.82	1.48	1.62
A1B-Avg	4.64	4.07	-4.49	-4.48	-3.23	-3.04	1.43	0.79	-4.13	-3.91	1.60	1.41
Dry extremes: Change in the exceedance frequency of SPI/mRAI < -1.5 [%]												
CLM R1	-10.48	-8.31	19.29	17.83	-0.48	-0.24	-7.50	-7.14	10.95	10.31	-10.36	-10.36
CLM R2	-4.29	-5.34	23.69	22.50	3.33	4.14	-2.74	-3.55	15.24	12.72	-6.07	-6.14
REMO R1	5.96	5.90	19.52	18.12	-0.96	-1.66	-2.94	-3.31	17.89	17.11	-4.39	-4.89
WX-nor	4.00	3.40	23.83	27.77	5.67	5.87	-4.77	-2.87	15.17	13.92	11.53	6.73
WX-dry	6.50	7.63	20.50	21.08	2.17	1.01	-8.66	-8.28	23.33	22.90	-8.14	-7.12
WX-wet	7.33	7.20	32.83	33.29	-1.17	-4.23	-4.03	-3.59	33.00	31.27	-5.08	-5.91
WG06-nor	-1.85	-3.12	16.67	14.66	16.67	13.26	5.48	8.17	18.15	16.19	5.50	4.02
WG06-dry	0.19	-1.48	24.26	29.71	29.07	29.27	-6.90	-6.13	20.37	20.52	2.08	1.97
WG06-wet	7.41	7.78	15.00	16.05	4.44	5.74	0.24	0.66	15.37	20.04	4.66	1.20
WG10-Avg	1.87	1.56	20.47	21.81	5.01	4.78	9.41	9.12	18.51	18.92	7.31	6.85
WG10-Min	-4.62	-5.25	6.35	6.70	-4.49	-4.31	1.20	0.79	7.82	7.92	1.70	1.03
WG10-Max	6.09	6.68	34.87	37.49	15.58	16.06	26.26	27.68	43.40	44.47	23.00	22.61
A1B-Avg	1.66	1.56	21.17	21.52	4.88	4.41	-0.97	-0.71	18.26	17.83	-0.36	-1.20

Trends are illustrated with colour coding (red = precipitation decrease/less wet extremes/more dry extremes, white = no change, blue = precipitation increase/more wet extremes/less dry extremes), with colour intensity illustrating trend magnitudes

Table 5 Same as in Table 4 but for monthly trends of wet and dry extremes

RCM		CLM -R1	CLM -R2	REMO -R1	WX-nor	WX-dry	WX-wet	WG06 -nor	WG06 -dry	WG06 -wet	WG10 -Avg	WG10 -Min	WG10 -Max	A1B-Avg
Wet extremes: Change in the exceedance frequency of SPI/mRAI > 1.5 [%]														
Jan	**SPI**	-0.4	0.0	1.3	2.3	-5.5	-6.0	-3.5	9.8	2.6	-4.3	-7.1	2.6	-0.7
	RAI	-0.5	-1.1	0.9	2.2	-8.0	-6.3	-3.6	4.6	3.4	-4.5	-7.6	-0.4	-1.4
Feb	**SPI**	-2.4	26.9	2.3	-3.5	1.2	-9.8	-4.4	9.1	-8.1	-4.7	-8.6	2.2	0.9
	RAI	-2.7	26.9	2.5	-3.3	2.9	-8.5	-4.7	6.1	-4.6	-4.8	-8.4	2.6	1.2
Mar	**SPI**	5.1	0.7	18.6	-4.7	-7.0	-4.0	0.6	3.7	7.8	-0.2	-4.9	7.9	4.0
	RAI	5.0	-1.8	21.7	-4.4	-6.3	-4.3	0.3	4.0	8.4	-0.6	-5.1	8.1	4.4
Apr	**SPI**	18.1	8.6	-1.2	4.0	-1.5	-2.0	1.9	-5.4	-0.9	-2.9	-7.4	1.4	1.6
	RAI	20.8	8.1	-2.1	3.4	-1.7	-5.1	1.2	-5.5	-1.9	-2.9	-6.3	1.4	1.2
May	**SPI**	2.3	4.9	0.6	2.7	-7.3	-3.0	-4.1	-0.2	4.4	-1.1	-5.7	1.9	0.1
	RAI	-0.4	4.3	-0.8	3.3	-7.3	-2.0	-4.2	-1.0	4.8	-1.0	-4.8	1.4	-0.4
Jun	**SPI**	-0.8	-2.4	-2.9	-0.2	-9.2	-4.8	-5.2	-8.1	-4.3	-1.8	-6.3	5.4	-3.4
	RAI	-0.9	-4.1	-3.4	-1.7	-7.7	-5.8	-6.4	-7.9	-3.7	-1.6	-5.9	5.7	-3.7
Jul	**SPI**	-3.6	0.4	3.9	-4.7	-5.2	-7.3	-1.9	-7.8	-0.6	-3.7	-10.7	1.3	-2.1
	RAI	-4.0	0.0	3.2	-4.0	-5.7	-4.8	-1.7	-7.5	0.2	-2.7	-7.1	1.5	-1.9
Aug	**SPI**	-3.8	1.5	-3.1	-1.5	-2.0	-5.8	0.0	-5.9	-1.3	-3.7	-6.0	4.8	-2.7
	RAI	-4.0	-2.0	-2.0	-0.9	-2.1	-4.6	0.1	-5.5	-0.9	-3.2	-6.3	4.2	-2.6
Sep	**SPI**	-6.9	-3.2	3.3	-1.2	-5.5	-5.0	-3.1	-5.9	5.2	-2.0	-8.5	3.7	-1.8
	RAI	-6.2	-3.8	3.0	-3.0	-6.1	-4.8	-3.6	-6.2	2.0	-1.8	-8.6	4.0	-2.2
Oct	**SPI**	3.7	-2.5	-0.7	-9.8	0.3	-2.2	0.2	5.4	-2.4	-0.9	-4.7	4.0	-0.8
	RAI	4.6	-2.3	-2.1	-8.0	-1.0	-1.6	-0.4	4.8	-2.6	-1.7	-4.8	2.5	-1.1
Nov	**SPI**	-0.1	0.4	-1.7	-0.2	-8.3	-9.5	0.7	-3.3	-3.7	-1.1	-6.4	5.6	-2.1
	RAI	-0.3	1.5	-1.8	-0.3	-6.8	-9.8	1.1	-6.9	-5.1	-1.6	-7.1	5.5	-2.4
Dec	**SPI**	7.6	12.7	3.4	-3.3	5.0	9.0	-5.4	-1.7	-6.5	-6.5	-11.3	-2.4	1.2
	RAI	6.9	11.5	3.2	-2.8	4.7	9.7	-4.1	-5.1	-4.8	-5.9	-9.1	-3.4	1.1
Dry extremes: Change in the exceedance frequency of SPI/mRAI < -1.5 [%]														
Jan	**SPI**	-5.0	8.0	-6.6	-5.2	-1.5	-2.0	1.1	-8.0	-8.0	-1.4	-9.9	6.9	-2.9
	RAI	-6.1	7.8	-6.8	-5.8	-1.9	-4.7	1.7	-11.0	-8.3	-1.4	-10.2	8.0	-3.5
Feb	**SPI**	-3.1	-3.5	-6.4	-8.2	-2.2	-2.5	-0.4	-9.1	9.1	2.0	-6.9	18.3	-2.4
	RAI	-3.4	-3.6	-7.6	-9.1	-1.3	-2.9	1.6	-16.1	7.2	1.5	-9.4	17.4	-3.3
Mar	**SPI**	-4.2	-3.8	-7.3	0.8	1.8	1.7	-1.7	9.1	-3.1	0.7	-3.5	5.5	-1.5
	RAI	-4.3	-6.4	-7.0	2.5	-1.7	0.9	-2.5	9.4	-4.3	0.6	-3.9	6.3	-2.1
Apr	**SPI**	-7.0	1.4	-10.3	2.3	-1.3	0.2	1.9	0.9	2.0	4.7	-2.5	10.4	-1.3
	RAI	-6.8	1.5	-10.3	1.8	-2.1	-1.4	1.3	2.2	4.0	4.6	-3.7	11.1	-1.3
May	**SPI**	10.0	-1.7	11.9	-1.8	7.3	3.5	6.5	-5.6	-2.8	-0.8	-6.7	4.1	3.5
	RAI	10.7	-2.7	11.3	-3.7	7.5	3.9	6.3	-5.3	-4.5	-1.5	-7.1	3.9	3.0
Jun	**SPI**	11.0	10.6	20.6	4.3	11.0	15.0	10.7	19.4	11.9	8.1	1.7	14.4	12.7
	RAI	9.7	11.2	20.7	3.0	13.4	17.1	11.5	20.2	15.0	8.6	1.2	15.9	13.3
Jul	**SPI**	13.1	17.5	15.2	22.1	3.3	20.5	11.3	5.7	9.8	13.2	4.9	22.0	13.6
	RAI	13.7	18.3	14.8	23.3	2.3	23.0	12.7	7.1	11.0	14.4	3.3	23.7	14.3
Aug	**SPI**	21.1	11.1	14.8	12.3	6.8	9.7	0.4	13.1	17.0	15.4	4.4	27.1	13.2
	RAI	21.0	10.5	14.2	14.3	6.6	11.3	1.9	14.4	19.9	16.4	3.5	32.4	13.8
Sep	**SPI**	6.7	13.8	6.6	2.2	-2.5	1.5	5.2	6.7	6.5	1.9	-2.1	8.0	5.0
	RAI	6.3	12.7	7.6	3.4	-3.3	2.0	4.5	6.6	6.2	1.9	-2.1	7.9	5.1
Oct	**SPI**	-5.6	6.4	6.4	18.3	6.8	-9.5	5.4	16.3	11.3	2.9	-6.6	8.8	5.2
	RAI	-6.2	6.9	7.3	22.9	6.9	-10.0	5.5	15.9	12.0	2.4	-8.2	8.9	5.6
Nov	**SPI**	-7.7	-1.8	-2.0	-1.3	0.5	4.0	5.0	14.3	11.9	-0.9	-12.1	12.4	0.8
	RAI	-7.5	-2.5	-2.2	-3.4	0.2	3.8	4.2	14.4	11.3	-1.2	-12.9	12.7	0.3
Dec	**SPI**	-7.1	-7.4	-2.6	-6.3	-7.2	-11.8	-2.6	-6.9	1.1	6.1	-8.3	23.2	-3.0
	RAI	-10.0	-7.8	-2.7	-6.8	-8.2	-11.1	-3.2	-7.7	1.6	6.0	-8.0	22.5	-3.5

Table 6 Mann–Kendall trends for SPI-1 and mRAI-1, calculated for 12 regional climate projections under the SRES scenario A1B averaged over the study area for period 2001–2100

2001–2000		REMO	CLM 1	CLM 2	WEREX VI nor.	WEREX VI dry	WEREX VI wet	WETTREG 2006 nor.	WETTREG 2006 dry	WETTREG 2006 wet	WETTREG 2010 Avg.	WETTREG 2010 Min.	WETTREG 2010 Max.
Jan	SPI	0.62	0.24	-2.53	0.75	-1.44	-1.89	-0.36	4.90	2.45	-3.16	-5.46	0.23
	RAI	0.13	-0.52	-2.20	0.80	-1.80	-2.61	-0.99	3.47	1.82	-4.18	-6.78	-2.07
Feb	SPI	-0.25	0.33	4.83	0.49	-0.83	-2.03	-2.56	4.72	-1.00	-3.92	-6.73	-0.36
	RAI	0.10	1.22	6.06	0.67	-0.24	-2.48	-2.07	4.22	-1.49	-4.10	-6.92	-1.13
Mar	SPI	7.81	5.74	6.75	-1.20	-0.24	-0.20	1.54	1.04	3.54	-0.11	-2.11	2.00
	RAI	8.15	6.44	6.73	-1.14	-0.29	0.18	1.83	1.66	3.81	0.37	-2.29	2.48
Apr	SPI	4.46	6.81	3.10	1.01	0.35	1.69	1.87	-1.58	-0.67	-0.74	-2.95	2.14
	RAI	4.20	7.68	3.70	0.98	0.46	2.33	1.91	-0.96	-0.80	-0.81	-3.14	1.55
May	SPI	-1.86	-0.55	-0.19	-0.67	-2.64	-2.65	-0.81	2.91	-0.49	-1.05	-2.70	1.94
	RAI	-2.01	-0.98	0.07	-0.47	-2.99	-3.43	-1.21	2.41	-0.06	-1.60	-2.97	1.31
Jun	SPI	-2.21	0.13	-0.19	-2.53	-3.32	-3.11	-3.75	-5.88	-1.29	-1.37	-4.37	3.37
	RAI	-2.44	-0.14	-0.02	-2.31	-4.47	-3.32	-3.75	-6.34	-2.32	-1.47	-4.63	2.83
Jul	SPI	1.17	0.95	-0.24	-2.76	0.95	-1.47	-0.29	1.55	-0.18	-0.03	-0.80	1.86
	RAI	2.53	0.51	-0.27	-2.75	1.35	-2.14	-0.50	1.32	-0.30	0.29	-1.32	4.38
Aug	SPI	1.05	0.82	0.41	-0.49	1.76	0.81	2.88	0.48	-0.88	-0.15	-2.33	1.81
	RAI	1.57	1.67	1.45	-0.30	2.60	0.81	3.84	0.96	-0.53	1.61	-1.10	3.19
Sep	SPI	-2.65	-1.95	-2.38	-0.57	-2.67	-3.11	-5.62	-4.07	-1.34	-2.84	-5.19	-0.82
	RAI	-0.75	-1.31	-0.57	-0.64	-1.73	-2.39	-4.66	-3.45	-1.03	-2.75	-4.57	-1.81
Oct	SPI	7.32	6.80	3.04	-1.52	4.16	8.14	2.85	1.24	1.79	3.92	1.72	6.71
	RAI	7.50	8.07	3.93	-1.50	5.42	8.85	3.88	1.69	3.28	4.47	2.90	7.27
Nov	SPI	2.16	3.50	1.50	-0.04	-2.36	-0.59	-4.34	-5.96	-4.33	-0.55	-3.28	2.18
	RAI	2.18	3.61	2.53	-0.02	-2.57	-1.26	-3.96	-5.30	-3.83	-0.74	-3.87	2.64
Dec	SPI	3.15	3.81	6.59	0.77	4.82	4.93	3.84	3.65	3.86	-0.42	-3.98	3.41
	RAI	3.13	4.03	6.74	0.76	4.94	5.84	3.43	3.29	3.88	-0.77	-3.48	3.56

The background colour indicates the direction (blue, precipitation increase and orange, precipitation decrease) and the significance of the trends (the darker the colour, the higher the statistical significance; see below)

Significance level α 0.2 0.1 0.05 0.01 0.001

Positive trend direction

Negative trend direction

increasing evapotranspiration rates since rising temperatures potentially aggravate drought conditions. Thus, evaluations of future drought risk should include not only precipitation, but also other climate parameters—at least temperature. Related indices are the Palmer drought severity index (PDSI) (Palmer 1965), the

reconnaissance drought index (RDI) (Tsakiris and Vangelis 2005) and the standardised precipitation evapotranspiration index (SPEI) (Vicente-Serrano et al. 2010). The latter applies the same methodology as the SPI but uses the water balance (precipitation minus evapotranspiration) instead of precipitation as input variable. A log-logistic distribution function is used in the calculation procedure instead of the gamma distribution.

The RAI concept may be applied to the water balance (WB=$P-$ETP) similar to the SPEI, yielding a water balance anomaly index WBAI:

$$WBAI_i = \pm SF \cdot \frac{WB_i - \overline{WB}}{\bar{E} - \overline{WB}}, \quad (2)$$

where

WB_i	Monthly water balance of month i
$\overline{WB}$	Median monthly water balance of the validation period 1961–2000 for the respective month (e.g. if i is January, then $\overline{WB}$ is the median of all January water balance sums of the years 1961–2000)
$\bar{E}$	Mean of the 10 % most water balance sums (10 % percentile for positive anomalies, 90 % percentile for negative anomalies) of the validation period 1961–2000 for the respective month (e.g. if i is January, then $\bar{E}$ is the mean of the 10 % most extreme January water balance sums of the years 1961–2000)
$\pm SF$	Scaling factor (positive for $WB_i \geq \overline{WB}$, and negative for $WB_i <_n$)

The scaling factor may be different from the one applied for the mRAI. First, tests (not displayed here) show that WBAI and SPEI are similarly well comparable as mRAI and SPI have shown to be in this study, but further analyses are needed.

4 Conclusions

This study evaluated the use of a modified version of the Rainfall Anomaly Index (mRAI) as an alternative to the SPI in assessing future (extreme) precipitation conditions and trends in the temperate climate zone, using multi-model ensemble outputs. We analysed monthly and seasonal mRAI and SPI values for 12 regional climate projections in terms of absolute change signals, the statistical significance of trends and shifts in the frequency of precipitation anomaly classes with a focus on extreme events.

The mRAI is highly correlated with the SPI on monthly and seasonal timescales. Although this relationship is not completely linear and slight (non-significant) deviations in the frequency distributions may result, the magnitude and statistical significance of observed and projected trends are barely affected. SPI and mRAI deliver a similar spread and mean of all ensemble members, regarding the frequency of certain anomaly classes on timescales of 1 to 12 months. Taking into account the large bandwidth of change signals of individual regional climate projections, we assume that the mRAI provides sufficiently robust results for the evaluation of future precipitation anomaly trends for climate change adaptation purposes. The notably more complex calculation of the SPI bears no relevant advantages for this application. An analysis of a worldwide climate dataset would be needed to extend these conclusions to other climate zones.

For a specific evaluation of the future drought risk, purely precipitation-based indices like the tested SPI and mRAI bear some limitations and tend to underestimate the real drought risk. Rising temperatures potentially increase evapotranspiration rates, and thus may aggravate drought conditions. Thus future drought conditions should be evaluated using indices such as the Palmer index or the SPEI that also include temperature and evapotranspiration, respectively. Here, the application of the RAI concept on the water balance may be a similarly effective, robust and computationally less demanding alternative.

Acknowledgments This work was supported by the German KLIMZUG project REGKLAM (support code FKZ 01LR0802) and funded by the Federal Ministry of Education and Research (BMBF). The joint research project REGKLAM (Development and Testing of an Integrated Regional Climate Change Adaptation Programme for the Dresden Region; http://www.regklam.de) addresses the regional scale of climate change impacts and adaptation. We thank Anne Marie de Grosbois for her help with language editing and three anonymous referees for their helpful comments.

References

Bernhofer C, Matschullat J, Bobeth A (eds) (2009) Das Klima in der REGKLAM-Modellregion Dresden. Rhombos, Berlin

Bernhofer C, Matschullat J, Bobeth A (eds) (2011) Klimaprojektionen für die REGKLAM-Modellregion Dresden. Rhombos, Berlin

Easterling DR, Meehl GA, Parmesan C, Changnon SA, Karl TR, Mearns LO (2000) Climate extremes: observations, modeling, and impacts. Science 289:2068–2074. doi:10.1126/science.289.5487.2068

Enke W, Küchler W, Sommer W (2001) Klimaprognose für Sachsen - Regionalisierung von Klimamodell-Ergebnissen mittels des statistischen Verfahrens der Wetterlagen-Klassifikation und nachgeordneter multipler Regression für Sachsen. Report to the Saxon State Agenvy for Environment and Geology, Meteo-Research, Potsdam

Enke W, Schneider F, Deutschländer T (2005) A novel scheme to derive optimized circulation pattern classifications for downscaling and forecast purposes. Theor Appl Climatol 82:51–63. doi:10.1007/s00704-004-0116-x

Fink AH, Brücher T, Krüger A, Leckebusch GC, Pinto J, Ulbrich U (2004) The 2003 European summer heatwaves and drought –

synoptic diagnosis and impacts. Weather 59:209–216. doi:10.1256/wea.73.04

Guttman NB (1998) Comparing the Palmer drought index and the standardized precipitation index. J Am Water Resour Assoc 34:113–121

Guttman NB (1999) Accepting the standardized precipitation index: a calculation algorithm. J Am Water Resour Assoc 35:311–322

Hayes MJ, Svoboda MD, Wilhite DA, Vanyarkho OV (1999) Monitoring the 1996 drought using the standardized precipitation index. Bull Am Meteorol Soc 80:429–438

Hayes M, Svoboda M, Wall N, Widhalm M (2011) The Lincoln declaration on drought indices: universal meteorological drought index recommended. Bull Am Meteorol Soc 92:485–488. doi:10.1175/2010BAMS3103.1

Heinrich G, Gobiet A (2012) The future of dry and wet spells in Europe: a comprehensive study based on the ENSEMBLES regional climate models. Int J Climatol 32:1951–1970. doi:10.1002/joc.2421

Hollweg H-D, Böhm U, Fast I, Hennemuth B, Keuler K, Keup-Thiel E, Lautenschlager M, Legutke S, Radtke K, Rockel B, Schubert M, Will A, Woldt M, Wunram C (2008) Ensemble simulations over Europe with the Regional Climate Model CLM forced with IPCC AR4 Global Scenarios. Max Planck Institute for Meteorology, Hamburg

Jacob D, Podzun R (1997) Sensitivity studies with the regional climate model REMO. Meteorol Atmos Phys 63:119–129

Jacob D, Göttel H, Kotlarski S, Lorenz P, Sieck K (2008) Klimaauswirkungen und Anpassung in Deutschland-Phase 1: Erstellung regionaler Klimaszenarien für Deutschland. Final Report of the R&D project 20441138 to the German Federal Environmental Agency. 154

Karl TR, Nicholls N, Ghazi A (1999) Clivar/GCOS/WMO Workshop on Indices and Indicators for Climate Extremes Workshop Summary. Clim Chang 42:3–7. doi:10.1023/A:1005491526870

Kendall M (1970) Rank correlation methods, 4th edn. Griffin, London

Keyantash J, Dracup JA (2002) The quantification of drought: an evaluation of drought indices. Bull Am Meteorol Soc 83:1167–1180

Kottek M, Grieser J, Beck C, Rudolf B, Rubel F (2006) World map of the Köppen-Geiger climate classification updated. Meteorol Z 15:259–263

Kreienkamp F, Spekat A, Enke W (2010a) Ergebnisse eines regionalen szenarienlaufs für Deutschland mit dem statistischen Modell WETT REG2010. Report to the German Federal Environmental Agency. Climate & Environment Consulting Potsdam GmbH, Potsdam

Kreienkamp F, Spekat A, Enke W (2010b) Weiterentwicklung von WETTREG bezüglich neuartiger Wetterlagen. Climate & Environment Consulting Potsdam GmbH, Potsdam

Kundzewicz ZW, Radziejewski M, Pińskwar I (2006) Precipitation extremes in the changing climate of Europe. Clim Res 31:51–58

Lehner B, Döll P, Alcamo J, Henrichs T, Kaspar F (2006) Estimating the impact of global change on flood and drought risks in Europe: a continental, integrated analysis. Clim Chang 75:273–299. doi:10.1007/s10584-006-6338-4

Lloyd-Hughes B, Saunders MA (2002) A drought climatology for Europe. Int J Climatol 22:1571–1592. doi:10.1002/joc.846

Loukas A, Vasiliades L, Dalezios NR (2003) Intercomparison of meteorological drought indices for drought assessment and monitoring in Greece. Proc. Int. Conf. Environ. Sci. Technol. Lemnos Island, pp 484–491

Mann HB (1945) Nonparametric tests against trend. Econometrica 13:245–259. doi:10.2307/1907187

Manton MJ, Della-Marta PM, Haylock MR, Hennessy KJ, Nicholls N, Chambers LE, Collins DA, Daw G, Finet A, Gunawan D, Inape K, Isobe H, Kestin TS, Lefale P, Leyu CH, Lwin T, Maitrepierre L, Ouprasitwong N, Page CM, Pahalad J, Plummer N, Salinger MJ, Suppiah R, Tran VL, Trewin B, Tibig I, Yee D (2001) Trends in extreme daily rainfall and temperature in Southeast Asia and the South Pacific: 1961-1998. Int J Climatol 21:269–284. doi:10.1002/joc.610

McKee TB, Doesken NJ, Kleist J (1993) The relationship of drought frequency and duration to time scales. Eighth Conf Appl Climatol

McKee TB, Doesken NJ, Kleist J (1995) Drought monitoring with multiple time scales. 9th AMS Conf. Appl. Climatol. Dallas, Texas, pp 233–236

Moreira EE, Mexia JT, Pereira LS (2013) Assessing homogeneous regions relative to drought class transitions using an ANOVA-like inference. Application to Alentejo, Portugal. Stochast Environ Res Risk Assess 27:183–193. doi:10.1007/s00477-012-0575-z

Nakicenovic N, Swart R (eds) (2001) Special Report on Emissions Scenarios (SRES). Special Report of the Intergovernmental Panel on Climate Change. Cambridge Uni-versity Press, UK. 520

Nicholls N, Murray W (1999) Workshop on indices and indicators for climate extremes: Ashville, NC, USA, 3-6 June 1997 - Breakout Group B: Precipitation. Clim Chang 42:23–29

Palmer WC (1965) Meteorological drought. Weather Bureau Research Paper No. 45, US Deptartment of Commerce, Washington, DC. 58

Rebetez M, Mayer H, Dupont O, Schindler D, Gartner K, Kropp JP, Menzel A (2006) Heat and drought 2003 in Europe: a climate synthesis. Ann For Sci 63:569–577. doi:10.1051/forest:2006043

Roeckner E, Bäuml G, Bonaventura L, Brokopf R, Esch M, Giorgetta M, Hagemann S, Kirchner I, Kornblueh L, Manzini E, Rhodin A, Schlese U, Schulzweida U, Tompkins A (2003) The atmospheric general circulation model ECHAM5. Part I - model description. MPI Report, Max Planck Institute for Meteorology, Hamburg. 127

Roeckner E, Brokopf R, Esch M, Giorgetta M, Hagemann S, Kornblueh L, Manzini E, Schlese U, Schulzweida U (2004) The atmospheric general circulation model ECHAM5. Part II - Sensitivity of simulated climate to horizontal and vertical resolution. MPI Report, Max Planck Institute for Meteorology, Hamburg. 55

Roeckner E, Brokopf R, Esch M, Giorgetta M, Hagemann S, Kornblueh L, Manzini E, Schlese U, Schulzweida U (2006) Sensitivity of simulated climate to horizontal and vertical resolution in the ECHAM5 atmosphere model. J Clim 19:3771–3791. doi:10.1175/JCLI3824.1

Schönwiese CD, Staeger T, Trömel S (2004) The hot summer 2003 in Germany. Some preliminary results of a statistical time series analysis. Meteorol Z 13:323–327. doi:10.1127/0941-2948/2004/0013-0323

Schwarzak S, Hänsel S, Matschullat J (2014) Projected changes in extreme precipitation characteristics for Central Eastern Germany (21st century, model-based analysis). Int J Climatol. doi:10.1002/joc.4166

Spekat A, Enke W, Kreienkamp F (2007) Neuentwicklung von regional hoch aufgelösten Wetterlagen für Deutschland und Bereitstellung regionaler Klimaszenarios auf der Basis von globalen Klimasimulationen mit dem Regionalisierungsmodell WETTREG auf der Basis von globalen Klimasimulationen mit ECHAM5/MPI-OM T63 L31 2010 bis 2100 für die SRES-Szenarios B1, A1B und A2. German Federal Environmental Agency, Dessau-Roßlau

Tilahun K (2006) Analysis of rainfall climate and evapo-transpiration in arid and semi-arid regions of Ethiopia using data over the last half a century. J Arid Environ 64:474–487. doi:10.1016/j.jaridenv.2005.06.013

Tsakiris G, Vangelis H (2005) Establishing a drought index incorporating evapotranspiration. Eur Water 9:3–11

Ulbrich U, Brücher T, Fink AH, Leckebusch GC, Krüger A, Pinto JG (2003) The central European floods of August 2002: part 1 – rainfall periods and flood development. Weather 58:371–377. doi:10.1256/wea.61.03A

Van Rooy MP (1965) A Rainfall anomaly index (RAI) independent of time and space. Notos 14:43–48

Vicente-Serrano SM, Beguería S, López-Moreno JI (2010) A multiscalar drought index sensitive to global warming: the standardized

precipitation evapotranspiration index. J Clim 23:1696–1718. doi:10.1175/2009JCLI2909.1

Vidal J-P, Martin E, Kitova N, Najac J, Soubeyroux JM (2012) Evolution of spatio-temporal drought characteristics: validation, projections and effect of adaptation scenarios. Hydrol Earth Syst Sci 16:2935–2955. doi:10.5194/hess-16-2935-2012

WMO (2009) Lincoln declaration on drought indices. World Meteorological Organization (WMO) http://www.wmo.int/pages/prog/wcp/agm/meetings/wies09/documents/Lincoln_Declaration_Drought_Indices.pdf, last accessed 15 Dec 2014

Wu H, Svoboda MD, Hayes MJ, Wilhite DA, Wen F (2007) Appropriate application of the standardized precipitation index in arid locations and dry seasons. Int J Climatol 27:65–79. doi:10.1002/joc.1371

Zhang Q, Xiao M, Sing VP, Chen X (2013) Copula-based risk evaluation of droughts across the Pearl River basin, China. Theor Appl Climatol 111:119–131. doi:10.1007/s00704-012-0656-4